ACS OMEGA

Open Access

http://pubs.acs.org/journal/acsodf

Article

In Situ Ni(II) Complexation Induced Deprotonation of Bis-Thiourea-Based Tweezers in DMSO−Water Medium: An Approach toward Recognition of Fluoride Ions in Water with Organic Probe Molecules

Bikash Chandra Mushahary, Nishant Biswakarma, Ranjit Thakuria, Rituraj Das, and Sanjeev Pran Mahanta*

Cite This: *ACS Omega* 2024, 9, 29300−29309

Read Online

ACCESS | Metrics & More | Article Recommendations | Supporting Information

ABSTRACT: Recognition of fluoride in water through the fluoride-induced Brönsted acid−base deprotonation reaction of an organic probe molecule is still a challenging task owing to the lower basicity of fluoride ions and the instability of the conjugate base of the probe molecules in aqueous medium. Herein, we report a complementary strategy in which the conjugate base of the studied bis-thiourea molecule in dimethyl sulfoxide (DMSO) medium is simultaneously stabilized through chelation of the Ni(II) ion, which eventually facilitates the recognition of the fluoride ion in water samples. The recognition methodology is validated colorimetrically and electrochemically, and finally, the applicability of the approach is explored with water samples collected from fluoride-affected areas. The limit of detection value for the fluoride ion in water medium was found to be 0.2 and 0.3 ppm with UV−visible spectroscopy and differential pulse voltammetry measurements, respectively. The methodology is also demonstrated on a paper strip for the detection of the fluoride ion with the naked eye and a smartphone-based RGB sensor. The scheme has been shown to be effective in enhancing the aqueous fluoride recognition ability of the organic probe molecules with acidic hydrogen prone to deprotonation by the fluoride ion.

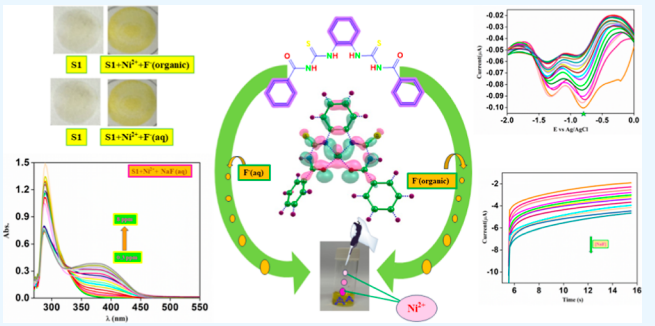

INTRODUCTION

Over the last few decades, significant efforts have been devoted to the design and synthesis of probe molecules for reliable and cost-effective detection of various environmental and medically important cationic and anionic species.[1−3] Among the anionic species, mineral fluoride (F^-) has drawn much attention due to its duplicitous role in human health.[3−7] Fluoride is known to improve dental health in humans and helps in the prevention of osteoporosis by stimulating osteoblast activity and inhibiting osteoclast activity.[3−10] The World Health Organization (WHO) recommended the maximum permissible limit of F^- in drinking water to be 1.5 mg/L.[11] Therefore, it is admissible to add fluoride into toothpaste, pharmaceutical agents, and even drinking water where the fluoride level in drinking water is lower than the WHO standard.[7] On the adverse side, prolonged over-exposure to fluoride can have detrimental effects on human health such as occurrences of dental and skeletal fluorosis, osteosarcoma, neurotoxicity during the prenatal development of child, resulting in a lower intelligent quotient, increased risk of attention-deficit/hyperactivity disorder, gastrointestinal disturbance, abdominal pain, salivation, bradycardia, tachycardia, etc.[12−16] The occurrence of F^- in soil and groundwater is mostly geogenic, but some anthropogenic industrial and agricultural activities are also accountable for large-scale fluoride contamination in water in certain regions.[17] Fluorosis is endemic in more than 25 countries across the globe including Asia, Africa, Europe, and North/South America.[17−19] Therefore, the treatment of water prior to human consumption is vital in these regions for public health benefits. Routine real-time monitoring and quantification of fluoride in drinking water under physiological conditions is necessary to decide where to add fluoride and where to install a defluoridation unit (DFU) and conduct timely replacement of the exhausted adsorbent bed of the DFUs. All these processes require timely monitoring of F^- in treated water in an easy manner, with minimal cost and high reliability.

Generally, methods such as the ion selective electrode (ISE), ion chromatography, inductively coupled plasma mass spectrometry, atomic absorption spectroscopy, inductively

Received: January 19, 2024
Revised: April 29, 2024
Accepted: May 7, 2024
Published: June 25, 2024

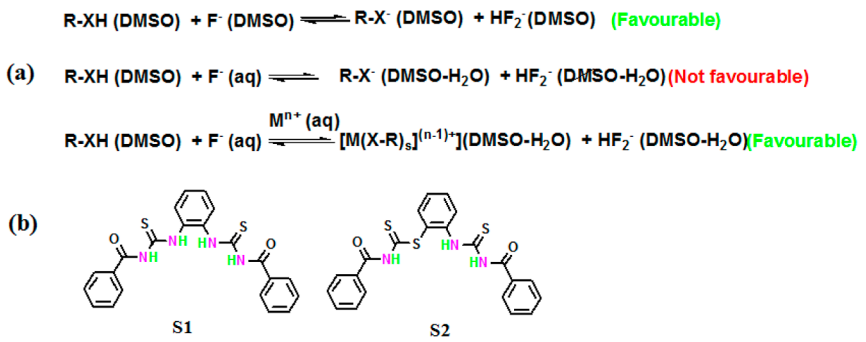

Figure 1. (a) Schematic representation of the idea behind the proposed methodology (X: O, N, and S; M: transition metal)and (b) structure of the probe molecule (**S1** and **S2**).

coupled plasma atomic emission spectroscopy, etc. are employed for precise quantification of F^- in water.[20] However, most of these methods involve sophisticated instrumentation requiring expertise knowledge and are not cost-effective for routine monitoring, specifically in remote areas. Among these, the ISE is relatively cost-effective and the most widely used for the assessment of the F^- ion in groundwater, but the presence of the Al(III) ion in water severely undermines the detection efficiency of F^- through the formation of an Al(III)−fluoride complex.[20,21] On the contrary, optical methods (colorimetric and fluorometric) are potential alternatives because of their easy operation and higher sensitivity.[22−30] The SPADNS-zirconium method has been one of the standard colorimetric estimation methods for the fluoride ion in aqueous medium. Although the performance of this method is satisfactory, the method is susceptible to interference by Al^{3+}, Cl^-, Fe^{3+}, SO_4^{2-}, and PO_4^{3-} ions, demanding the removal of the interfering ions from the sample prior to estimation.[20] In the attempt to develop a better colorimetric chemosensor for the fluoride ion, many probe molecules having acidic hydrogen have been reported as an optical sensor for selective detection of the F^- ion, which interact with the fluoride ion through H-bonding and Brönsted acid−base deprotonation reactions.[29−33] Most of these sensing strategies involve organic probe molecules, which demonstrate excellent sensitivity toward the fluoride ion in organic medium but unfortunately fail to show similar fluoride affinity in water medium. Fluoride has relatively high hydration energy and lower basicity in aqueous medium, leading to a lower dissociation constant for the fluoride-assisted deprotonation equilibrium of the probe molecule in aqueous medium.[34] All of these factors limit their applicability in aqueous medium. The literature is filled with a large number of organic probe molecules showing excellent sensitivity toward fluoride in organic medium but lacking sensitivity in water medium.[24,25] Therefore, it is noteworthy to develop a methodology applicable for the detection of the fluoride ion in water medium with the help of probe molecules that were already reported as a chemosensor for the fluoride ion in organic medium. This would lower the hurdles faced during the search of new chemosensor probe molecules as the synthesis of the new molecules involves standardization of a complex synthetic protocol. Several anion binding organic receptors having amide, urea, thiourea, pyrrole, indole, and guanidium functionalities capable of forming H-bonds and sometimes followed by deprotonation with the fluoride ion have been studied in the attempt to develop a chemosensor for the recognition of the fluoride ion. Furthermore, to improve the fluoride ion selectivity, the concept of preorganization along with the size of the binding cavity has also been explored with structures like macrocycles, clefts, etc.[34−41] As these receptors are mostly organic, they show good selectivity and sensitivity toward tetra alkyl salts of the fluoride ion in organic medium. However, their sensitivity drops abruptly even in the presence of a small amount of water, and hence, recognition of fluoride in aqueous medium by the same receptors is still a challenge. The presence of water in the reaction medium shifts the deprotonation equilibrium toward the protonated probe molecule, and hence, it is envisaged that stabilization of the deprotonated species by in situ metal complexation might favor the equilibrium toward right (Figure 1).[42−44] Herein, we have demonstrated a simple methodology with the help of two preorganized bis-thiourea functionalized tweezers (**S1** and **S2**), by which the fluoride sensitivity of the organic probe molecules can be retained in aqueous medium (Figure 1). It is found that the fluoride-induced colorimetric response of the tweezers persists to a significant extent upon the addition of water in the presence of the Ni(II) ion. The mechanism of the process was studied with ^{1}H NMR titration and electrochemical techniques, and an in-depth understanding of the processes involved was accomplished via density functional theory (DFT) calculations. The utility of the methodology was studied by monitoring the sensing performance with the help of UV−vis spectroscopy and differential pulse voltammetry (DPV) techniques. The applicability of the proposed methodology is also investigated with the cellulose paper platform as a paper sensor probe for detecting the fluoride ion in drinking water. It is quite remarkable that with our methodology, we were successfully able to detect the fluoride ion in real samples collected from fluoride-affected areas of Japarajan, Karbi Anglong district of Assam, India (longitude: 93.32143, latitude: 25.84665).

EXPERIMENTAL SECTION

The bis-thiourea tweezer type molecules **S1** and **S2** considered for study were prepared by following literature reported methods.[45] The probe molecules were characterized using Fourier transform infrared (FT-IR) spectroscopy, ^{1}H NMR, ^{13}C NMR, mass spectroscopy, and single crystal X-ray diffraction (SCXRD). Single crystals of both the receptors were generated from solution crystallization by slow evaporation of solvent. The fluoride recognition studies were performed by UV−vis spectrometry and cyclic voltammetry. Furthermore, the computational studies were done with the Gaussian 09 package.

https://doi.org/10.1021/acsomega.4c00624
ACS Omega 2024, 9, 29300−29309

RESULTS AND DISCUSSION

Structural Characterization of the Probe Molecules. Single crystals of both receptors were generated from solution crystallization by slow evaporation of solvent, which results in two polymorphic forms of **S1**. Single crystals of **S1** obtained from ethanol solvent (hereafter termed as Form 1) was solved in the triclinic $P\bar{1}$ space group containing one molecule in the asymmetric unit. Structural analysis exhibits a tweezer type conformation with the presence of two intramolecular N−H···O hydrogen bonds between the two independent thiourea N−H functionals and the benzoyl carbonyl moieties. In the 3D representation, one of the tweezer arms is stacked over neighboring molecules using $\pi\cdots\pi$ interactions between the terminal benzene ring and thiourea moiety as shown in (Figure 2). During attempted complexation with nickel salt, a polymorphic form of **S1** was obtained (hereafter designated as Form 2), which also was solved in the triclinic $P\bar{1}$ space group. Structural analysis shows the presence of two independent molecules in the asymmetric unit. Similar to the previous form, Form 2 also contains two intramolecular N−H···O hydrogen bonds between the thiourea and carbonyl moieties. In the 3D representation, the two independent molecules are further connected to each other using the N−H···O hydrogen bond between N−H and the carbonyl group of neighboring units, forming an infinite chain along the *a*-axis (Figure 2). Interdigitated parallel chains result in a 3D packing arrangement, as shown in Figure 2. The SCXRD structure of **S2** revealed the presence of intramolecular intrastrand N−H···O hydrogen bonding along with the interpenetration of one arm in the cleft of another **S2** through $\pi-\pi$ interaction, dictating the 3D packing.

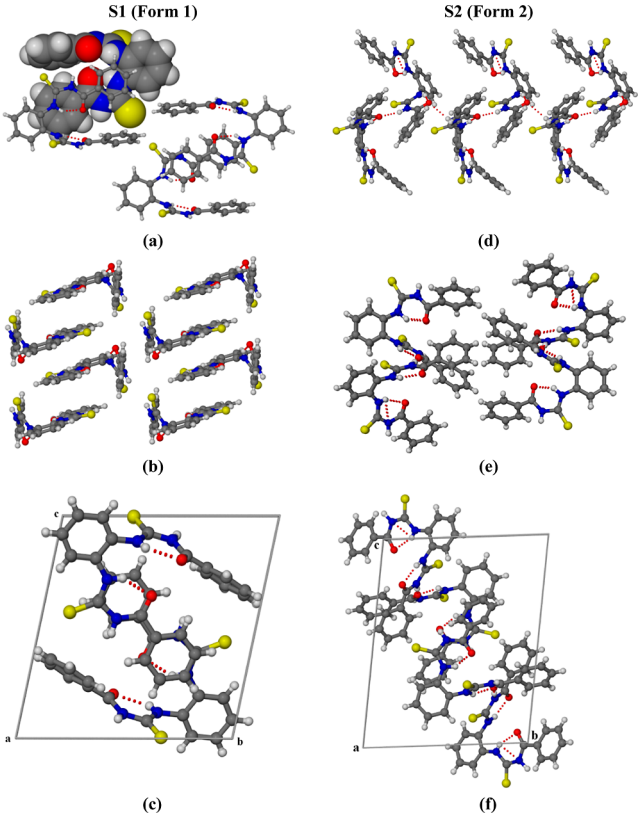

Figure 2. (a−c) $\pi\cdots\pi$ stacking arrangement of the **S1** molecule in Form 1 results in a 3D packing arrangement. No strong intermolecular hydrogen bonds have been observed between neighboring molecules; (d−f) an interdigitated infinite chain is formed using the N−H···O hydrogen bond between symmetry independent **S1** molecules in Form 2.

Anion Affinity Study of S1 and S2 in Organic Medium. The preliminary anion affinity of the probe molecules in the dimethyl sulfoxide (DMSO) medium was analyzed with the help of UV−vis spectroscopy. The UV−vis spectrum of the colorless solution of both **S1** and **S2** in DMSO medium showed absorbance at 270 nm and 290−320 nm, respectively. The anion binding affinity of the tweezers (**S1** and **S2**) was studied by monitoring the change in the UV−vis spectrum of the probe solution in DMSO (6×10^{-5} M) upon addition of the tetrabutylammonium salt solution of the anions (F^-, Cl^-, Br^-, I^-, ClO_4^-, HSO_4^-, $H_2PO_4^-$, and CH_3COO^-). Both the receptors showed affinity toward fluoride and acetate anions and correspondingly depict a change in the color of the solution to yellow. Probe **S1** resulted in the appearance of a new sharp peak at 340 nm upon interaction with F^- and CH_3COO^- ions. Similarly, **S2** in DMSO solution exhibited the emergence of the new peak at 370 nm upon the addition of the F^- ion and CH_3COO^- ion (Figure 3). For both **S1** and **S2**, the color change is distinct with fluoride in comparison to that with the acetate ion. Titration of **S1** with the fluoride ion in DMSO medium revealed a decrease in the intensity of the peak at 270 nm accompanied by a concomitant increase in the absorbance of the peak at 340 nm. Similarly, **S2** shows a continuous decrease in the intensity of the broad peaks at 290−320 nm along with the increase in the intensity of the peak at 370 nm by maintaining an isosbestic point at 335 nm (Figure 4). Job's plot analysis showed a plateau at 0.5, indicating 1:1 stoichiometry for the interaction of **S1** and **S2** with fluoride (Figure S12). The binding constants of the interaction of the probe molecules with the F^- ion were further calculated by the Benesi−Hildebrand plot and found to be 1.83×10^3 and 6.89×10^3 M^{-1}, respectively (Figure S13).[46]

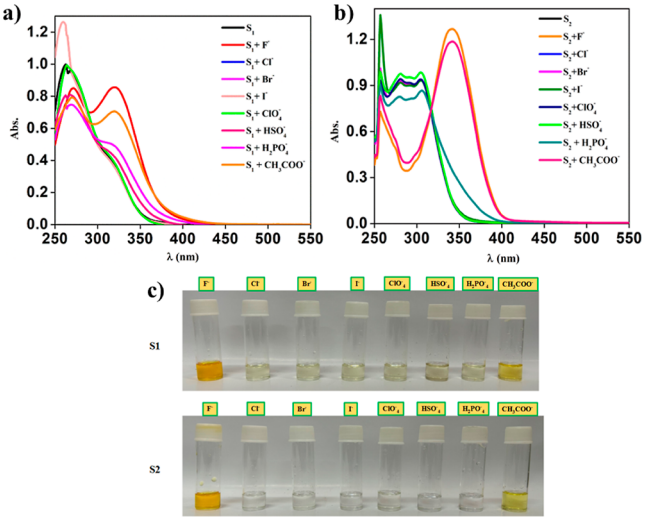

Figure 3. UV−vis spectra of probe molecule solution (6×10^{-5} M) in DMSO in the presence of different anions (5×10^{-3} M) (a) probe **S1** and (b) probe **S2** and (c) change in color of the probe molecules in the presence of different anions.

After successfully demonstrating the fluoride affinity of both **S1** and **S2** in organic medium, the affinity of both the probe molecules toward aqueous fluoride ions was investigated by

https://doi.org/10.1021/acsomega.4c00624
ACS Omega 2024, 9, 29300−29309

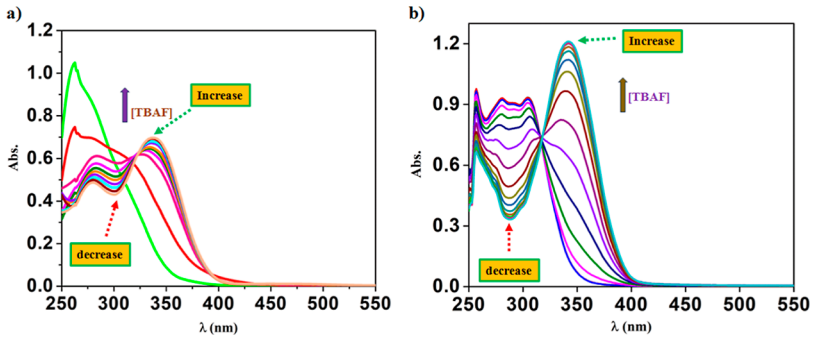

Figure 4. (a) Change in UV−vis spectra of **S1** [6×10^{-5} M] solution upon gradual addition of TBAF [10×10^{-3} M] in DMSO solution and (b) change in the UV−vis spectra of **S2** [6×10^{-5} M] solution upon gradual addition of TBAF [10×10^{-3} M] in DMSO solution.

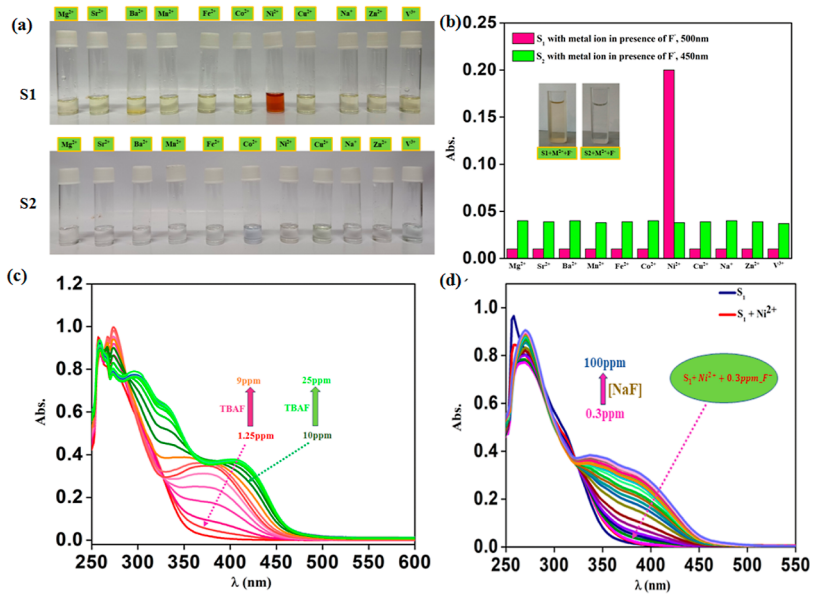

Figure 5. (a) Change in color of the probe molecule solution (1×10^{-3} M in DMSO) in the presence of aqueous solution of F^- and different metal salts (NaCl, $MgSO_4$, VCl_3, $MnCl_2$, $FeSO_4$, $CoCl_2$, $NiCl_2{\cdot}6H_2O$, $CuCl_2{\cdot}2H_2O$, $ZnCl_2$, $SrCl_2$, and $BaSO_4$); (b) bar representation of the relative changes in absorbance of **S1** and **S2** (6×10^{-5} M) in DMSO solution upon the addition of fluoride; (c) UV−vis titration of **S1** (6×10^{-5} M) in DMSO with varying concentrations of TBAF (10 mM) in the presence of aqueous Ni^{2+} ions (10 mM); and (d) UV−vis titration of **S1** (6×10^{-5} M) in DMSO with varying concentrations of aqueous NaF (10 mM) in the presence of 50 μL of 10 mM aqueous Ni^{2+} solution.

adding 300 μL of 10% (V/V) water to the solution of **S1**·F^- and **S2**·F^- in 3 mL of DMSO. It was observed that the color of the solution fades away and the absorbance of the peak in the visible region corresponding to the color diminishes (Figure S14). Furthermore, addition of aqueous solution of NaF to both the probe (**S1** and **S2**) solutions did not show any remarkable affect in the UV−vis spectra, indicating their inability to interact with the fluoride ion in the presence of water (Figure S15).

Fluoride Recognition Studies of S1 and S2 in Water Medium. In order to develop a strategy to make the colorimetric response of the studied tweezers toward the fluoride ion persistent in water medium, the deprotonation equilibrium of the probe molecules with aqueous fluoride ions were studied in the presence of transition metal ions. It is anticipated that the in situ transition metal complexation might also reinforce the colorimetric sensing response by improving the colorimetric change due to metal to ligand or ligand to metal charge transfer (LMCT) transitions. In this study, the metal salts that do not have any affinity toward the probe molecule (**S1** and **S2**) in the absence of the fluoride ion will be considered as being suitable for the purpose. Chloride and sulfate salts of the metal ions were chosen for the study as both the probe molecules did not show any affinity for both the counteranions.

The affinity of both the probe molecules toward metal ions was investigated by monitoring the UV−vis spectrum of the solution of **S1** and **S2** in DMSO (6×10^{-5} M) by adding 10 mM aqueous solution of the following metal salts NaCl, $MgSO_4$, VCl_3, $MnCl_2$, $FeSO_4$, $CoCl_2$, $NiCl_2{\cdot}6H_2O$, $CuCl_2{\cdot}2H_2O$, $ZnCl_2$, $SrCl_2$, and $BaSO_4$. It is found that both **S1** and **S2** did not show any affinity for the tested metal salts (Figure S17). Subsequently, the UV−vis spectrum of **S1** and **S2** in DMSO solution was recorded upon the addition of the above-mentioned metal salt solution in the presence of aqueous solution of fluoride ions (10×10^{-3} M). It was observed that upon the addition of Ni(II) salt to **S1** solution in the presence of fluoride, the color of the solution changed from colorless to red. However, no substantial color change was observed upon the addition of other aqueous metal salt solutions to **S1** in the presence of fluoride (Figures 5 and S18). Furthermore, reversing the order of addition of Ni(II) salt and aqueous

https://doi.org/10.1021/acsomega.4c00624
ACS Omega 2024, 9, 29300−29309

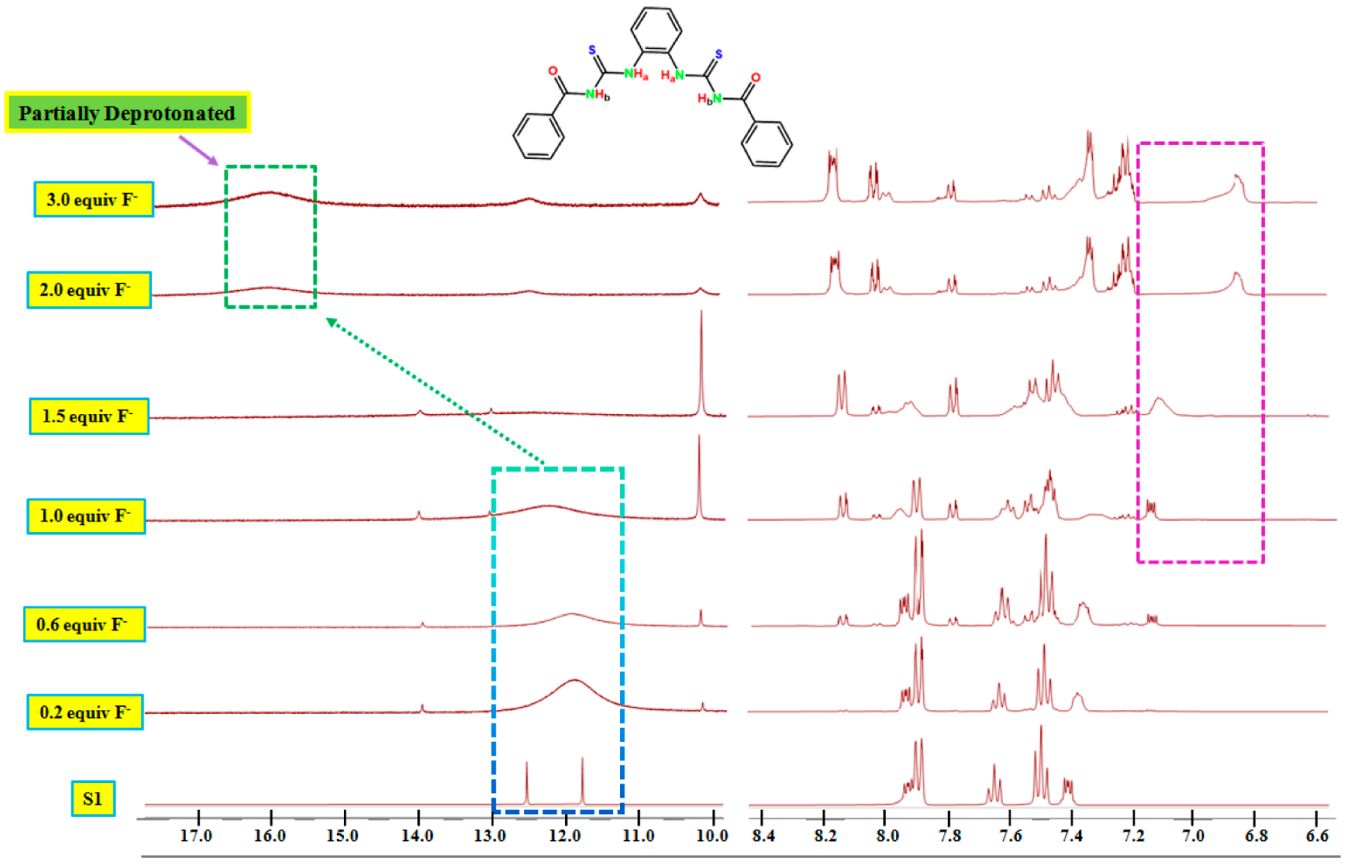

Figure 6. Change in the proton ^{1}H NMR spectrum of receptor **S1** upon titration with the F^- ion in DMSO-d_6 medium.

fluoride salt solution to **S1** produces a similar colorimetric output (Figure S20). Similarly, the fluoride binding affinity of **S2** in aqueous medium was also checked in the presence of the different metal salts. However, **S2** did not show any significant response toward the fluoride ion in water medium even in the presence of metal ions (Figure 5). This observation confers that among the two studied probe molecules, **S1** shows potential propensity to be used as a probe molecule toward sensing of fluoride ions in water medium in the presence of $NiCl_2$, and hence, molecule **S1** was considered for further study.

Gradual addition of an aqueous solution of TBAF to **S1**·Ni(II) solution in a DMSO−H_2O mixture led to gradual evolution of the peak at λ_{max} 380 nm by maintaining an isosbestic point at 328 nm. However, addition of TBAF beyond 10 ppm concentration triggers a bathochromic shift of the peak to 409 nm with a concomitant change of the isosbestic point to 363 nm (Figures 5c and S23). On the same note, titration of **S1**·Ni(II) solution in DMSO−H_2O medium with aqueous solution of NaF led to the emergence of the broad peak at 330−450 nm, whose intensity increases with the addition of NaF (Figures 5d and S19). Additionally, it was observed that 0.3 ppm aqueous fluoride can lead to an appreciable change in the UV−vis spectrum of **S1** in the presence of Ni(II) salt. The UV−vis experiments unequivocally conferred that probe molecule **S1** can be used as a colorimetric sensing probe toward the fluoride ion in aqueous medium in the presence of the Ni(II) ion. The optimum concentrations of **S1** and $NiCl_2$ to be used in the detection of the fluoride ion in water medium is determined and found as the mixture of 3 mL solution of **S1** (6.7×10^{-5} M) in DMSO and 50 μL solution of $NiCl_2$ (10 mM) in water. The change in absorbance at 380 nm wavelength of the probe solution [**S1** and Ni (II) in DMSO−H_2O mixture] fitted linearly with the increase in the concentration of the fluoride ion. The limit of detection (LOD) was calculated using the formula $3.3 \times S_D/m$, where S_D is the standard deviation of the blank and m is the slope of the calibration plot in the presence of metal ions.[47] The calculated LOD of the probe molecule **S1** in the presence of Ni(II) salt is calculated to be 0.2 ppm. Furthermore, Al^{3+} and Fe^{3+}, which are generally the most potential interfering ions in the SPADNS and ion selective method, did not show any significant change in the colorimetric response of this strategy (Figure S24).

Elucidation of the Fluoride Recognition Mechanism. To decipher the molecular level understanding of the recognition phenomenon, ^{1}H NMR titration was performed. It is observed that upon the addition of fluoride ion solution to **S1** in DMSO-d_6 medium, initially, the signals at 12.5 ppm for H_a and 11.75 ppm for H_b corresponding to the thiourea N−Hs become broad and almost disappear upon the addition of 1.5 equivalent of fluoride. Further addition of fluoride led to the reappearance of the peaks at 12.2 and 13.65 ppm along with a new broad peak at 16 ppm corresponding to the HF_2^- ion (Figure 6). Concomitantly, some of the phenyl ring proton shifted to the upfield region, indicating an increase in the electron density in the phenylenediamine unit, and some shifted to the downfield region, indicating a decrease in the electron density in the benzoyl phenyl moiety, upon interaction with fluoride. These observations pointed to the partial deprotonation of the N−H protons by the fluoride ion as the remaining two N−Hs are involved in the intramolecular

https://doi.org/10.1021/acsomega.4c00624
ACS Omega 2024, 9, 29300−29309

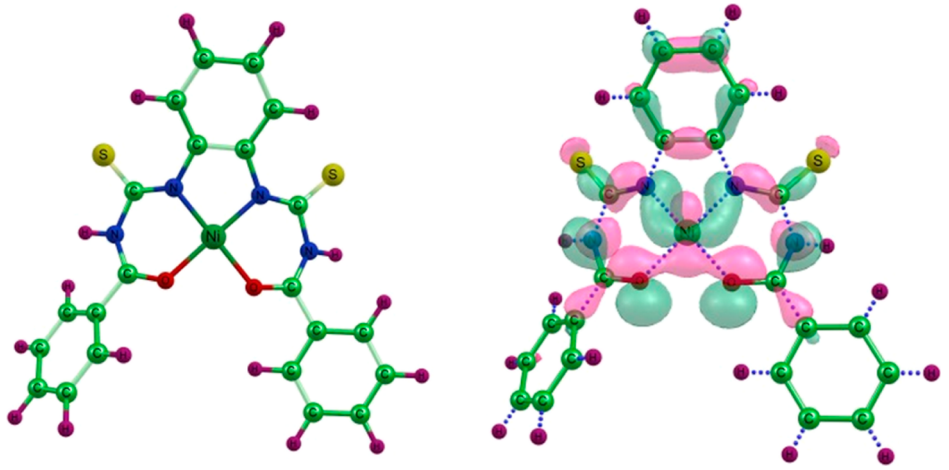

Figure 7. DFT optimized structure of the deprotonated [Ni(**S1**)] complex (left) and image of the HOMO−13 orbital representing the interactions involved (right).

H-bonding with the carbonyl oxygen of the benzoyl moiety. Therefore, from the ^{1}H NMR study, it is conferred that the recognition of fluoride by the probe molecule **S1** involves the Brönsted acid−base deprotonation reaction, which eventually might have led to the creation of favorable coordination sites for Ni(II) complexation. To elucidate the binding pattern of Ni(II) with **S1**, the metal complex was isolated as a red colored solid. The FT-IR spectra showed the bands at 530, 681, and 837 cm^{-1} corresponding to N−Ni−N asymmetric, O−Ni−O asymmetric, and O−Ni−N stretching vibrations, respectively.[48] This observation indicates the NiN_2O_2 coordinating pattern of the [Ni**S1**] complex (Figure S26). Furthermore, to reveal the oxidation state of the Ni(II) species in the reaction medium, an electron spin resonance (ESR) study was performed with the frozen mixture of **S1**, Ni(II) salt, and F$^-$ ions in DMSO medium. ESR spectra revealed the diamagnetic nature of the in situ Ni(II) complex formed during the sensing process (Figure S27). Unfortunately, we did not achieve success in isolating single crystals for the red Ni(II) complex.

In the effort to better understand the structure and nature of the electronic transitions exhibited by the [Ni**S1**] complex, DFT calculations using the Gaussian 09 package using the WB97XD/6-31++G(d,p) level of basis set was performed.[49] The singlet excited state was optimized using time-dependent DFT calculations, and the effect of solvation is considered by using the inbuilt conductor-like polarizable continuum model in the Gaussian 09 package.[49−52] The two possible deprotonation modes of **S1** were considered for the study, and the more favorable deprotonation was found for the thiourea N−H located near the benzoyl group due to the electron withdrawing nature of the benzoyl group (Figure S36). The optimized structure further revealed the intramolecular H-bonding interaction between the remaining pair of thiourea N−Hs with the benzoyl moiety. The optimized structure showed planar $[NiN_2O_2]$ η^4-bridging coordination of Ni with the deprotonated thiourea nitrogens and the two benzoyl oxygens. To enhance our confidence on the presence of Ni−N and Ni−O bonding in the complex, we carried out natural bond orbital (NBO) calculation of the complex. The HOMO−13 molecular orbital of the complex shows electron densities around the Ni atom spread over the coordinating N and O atoms (Figure 7). This further paves the way for the formation of Ni−O and Ni−N bonds with a significant exchange of electron density among them. However, the NHs that are being deprotonated were found to be different in the presence of Ni(II). The computed UV−vis spectrum of [**NiS1**] matches well with the experimental one, and the transition resulted from the HOMO to LUMO transitions. The frontier molecular orbitals derived from the NBO calculation revealed the intraligand charge transfer and the LMCT transition, which eventually led to the colorimetric response (Figure 7). The theoretical study also supported that the in situ Ni(II) complexation of deprotonated **S1** basically favors the fluoride-induced deprotonation reaction in aqueous medium and also reinforces the colorimetric response by favorable LMCT transition.

Electrochemical Recognition of the Fluoride Ion. To check whether the probe molecules can be used as electrochemical sensors for the aqueous fluoride ion, we have studied the redox behavior of the probe molecules in the presence of F$^-$ and Ni (II) ions. The cyclic voltammograms (CVs) of **S1** and **S2** were recorded from −2.0 to +1.5 V and −2.0 to +2.0 V, respectively, in the presence of Ni(II) salt upon gradual addition of the F$^-$ ion. The CV of **S1** in DMSO showed a pseudo reversible redox couple at −0.53 and −1.11 V, and the addition of tetrabutyl ammonium salt of fluoride to the solution resulted in the emergence of another oxidation peak at 1.27 V (Figure S28). However, addition of the aqueous solution of NaF did not lead to any significant change in the CV pattern, indicating the inertness of **S1** toward the fluoride ion in aqueous medium. A similar observation was also obtained with **S2** (Figure S29). However, addition of aqueous NaF solution to **S1** solution in the presence of Ni(II) showed a remarkable change in the CV, showing two oxidation peaks at −0.57 and 0.41 V and two reduction peaks at −0.81 and −1.62 V (Figure 6). The peaks at E_{pa} = −0.57 V and E_{pc} = −0.81 V represent the redox couples Ni(II)/Ni(I) and Ni(I)/Ni(II), respectively, whereas the peaks at E_{pa} = 0.41 V and E_{pc} = −1.61 V indicate the redox couples Ni(III)/Ni(I) and Ni(I)/Ni(III), respectively.[53,54] This observation suggested the in situ Ni(II) complexation of the conjugate base of **S1**, which is formed upon the deprotonation reaction with fluoride. However, **S2** did not show any significant response for aqueous sodium fluoride even in the presence of Ni(II) ions.[55,56]

Furthermore, the electrochemical response of **S1** upon incremental addition of aqueous fluoride ions in the presence

https://doi.org/10.1021/acsomega.4c00624
ACS Omega 2024, 9, 29300−29309

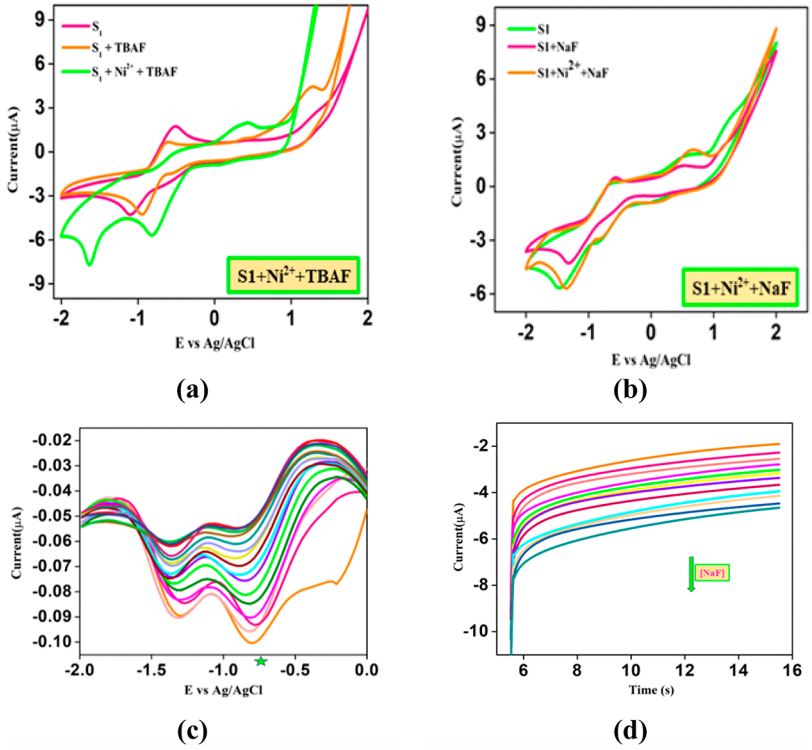

Figure 8. (a)CV of **S1** (5×10^{-5} M in DMSO) at 100 mV/s scan rate in the presence of TBAF (1 mM in DMSO) and Ni(II) (1 mM in water); (b) CV of **S1** (5×10^{-5} M) in the presence of NaF (1 mM in water) and Ni(II) (1 mM in water); (c) DPV plot the electrochemical response of **S1**·Ni(II) solution upon addition of NaF in aqueous medium; (d) chronoamperometric plot of probe **S1** with Ni^{2+}(aq) solution upon gradual addition of NaF (aq) solution [for the study, 30 mL of an **S1** solution in DMSO and 1 mL of a Ni^{2+} solution in water were considered].

of Ni(II) was studied with the DPV technique. The DPV curve was measured in the potential range of 0 to −2 V with a modulation amplitude of 10 mV, a modulation time of 50 s, steps of −30 mV, and the scan rate of 60 mV/s. It was observed that the reduction peak at −0.75 V (green star) shifted slightly toward the negative potential with a concomitant decrease in the peak current value upon the incremental addition of the aqueous fluoride ion (Figure 8c). The change in peak current shows a linear dependence $I_{pc} = 0.0062\,[NaF] - 0.06552$, $R^2 = 0.97918$ with the concentration of fluoride added (Figure S33). The linear dependency suggests that **S1** can be used as an electrochemical probe toward aqueous fluoride in the presence of Ni(II) salt. The concentrations of **S1** and $NiCl_2$ used for further study were 5×10^{-5} and 10×10^{-3} M in 40 mL of DMSO, respectively. The calculated LOD value for electrochemical sensing of fluoride by **S1** in the presence of Ni(II) was found to be 0.3 ppm.[57,58] The study also revealed that the acetate anion led to some responses similar to that of the fluoride anion but with lower intensity. However, comparatively lower basic anions like Cl^-, I^-, HSO_4^-, and $H_2PO_4^-$ did not show any significant effect on the DPV pattern (Figure S47). Chronoamperometric analysis also revealed the linear change in the current upon the incremental addition of an aqueous solution of NaF to **S1**·Ni^{2+} solution in a DMSO−H_2O mixture (Figure 8c). This study clearly revealed that the Ni(II)-mediated strategy can also be applicable in the electrochemical determination of fluoride in water medium.

Application in Paper Strips. The test strips were prepared using Whatman filter paper by making a spot of the probe molecule **S1**, by dropping 10 μL of a solution of **S1** (60 μM) in DMSO and 10 μL of an aqueous solution of $NiCl_2$ (10 mM) followed by air-drying for 15 min.[57,58] The test strips were placed on a glass plate, and 10 μL of different concentrations of F^- (0.5, 1, 1.5, 2, 3, 4, 5, 6, 7, and 8 ppm) was added (Figures 9a and S43). The color of the spots became yellow with varying intensity upon the addition of fluoridated water, which was clearly discernible with the naked eye. The RGB value of the spots was determined with the RGB color detector application developed by Raimon Gaspar Fernandez available in the Google play store. The RGB value shows a linear decrease in the percentage of the blue color index upon the increase in the concentration of fluoride (Table S3).

Detection of F^- in Real Samples. Finally, the methodology was validated by quantifying the fluoride ion concentration in water samples collected from the fluoride-affected area from Japarajan, Karbi Anglong district, Assam, India. It was observed that the water samples showed the representative colorimetric change from colorless to yellow, indicating the presence of fluoride ions. The concentration of fluoride ions was calculated from the calibration curve and obtained as 4.5 ppm (Figure 9). Furthermore, the DPV study also inferred the change in the peak current upon the addition of the water sample and revealed the presence of 4.8 ppm fluoride ions in the water sample. The results showed good agreement with the concentration obtained from the ISE measurement, which was found to be 5 ppm. The discrepancy in the results between our methodology and ISE measurement might be due to the interference from the other ions present in the sample. This observation clearly depicts that the demonstrated methodology can qualitatively and quantitatively define the presence of fluoride ions in aqueous medium.

https://doi.org/10.1021/acsomega.4c00624
ACS Omega 2024, 9, 29300−29309

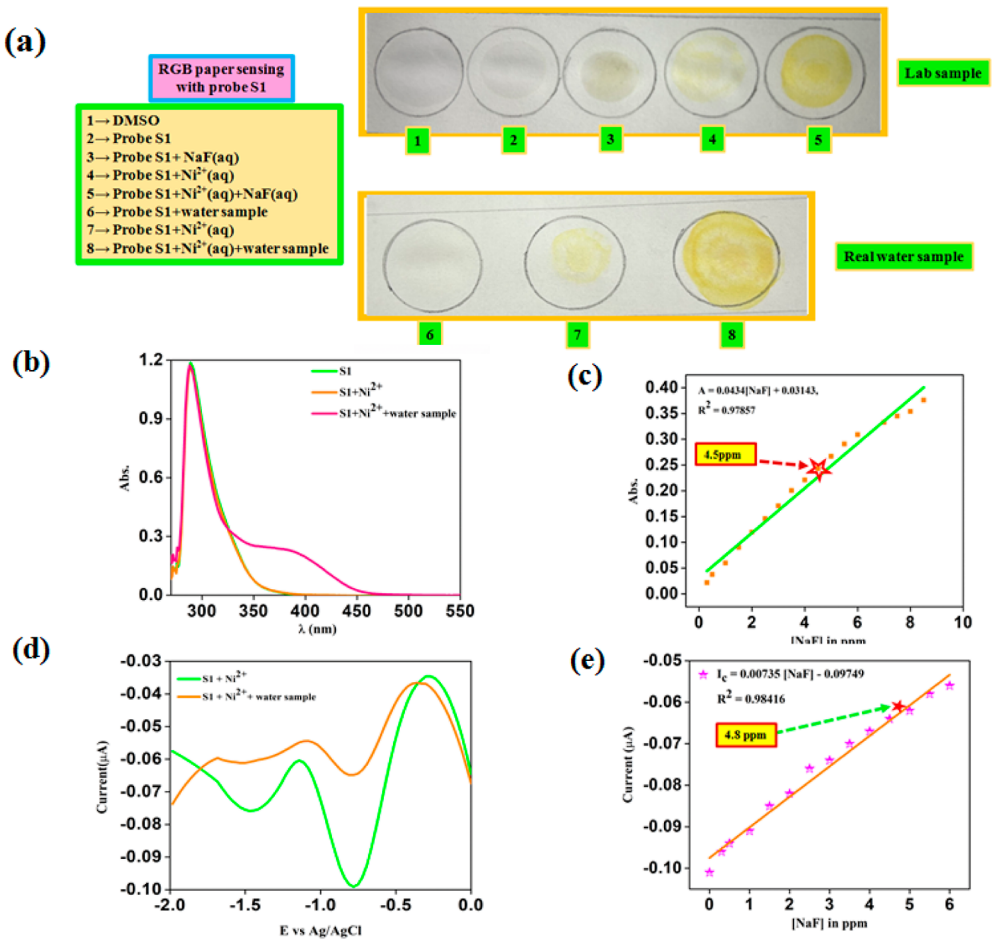

Figure 9. (a) Photograph of the colorimetric change of the test strips upon sequential addition of all the components, (b) UV−vis spectra plot of **S1** [6×10^{-5} M] in DMSO (3 mL) with the water samples (100 μL) collected from fluoride-affected areas in the presence of 50 μL of 10 mM aqueous Ni^{2+} ion, (c) calibration curve showing the change in absorbance with the increase in concentration of F^-; *: denotes the absorbance upon addition of water samples collected from fluoride-affected areas; (d) DPV pattern of **S1** with water samples collected from fluoride-affected areas in the presence of aqueous Ni^{2+} ions [10 mM]; and (e) calibration curve showing the change in current with the increase in concentration of F^-; *: denotes the absorbance upon the addition of water samples collected from fluoride-affected areas.

CONCLUSIONS

A Ni(II)-mediated strategy has been demonstrated for sensitive and selective colorimetric recognition of inorganic fluoride ions with probe molecule **S1** in water medium with bis-thiourea-based probe molecules. The methodology is further verified with electrochemical techniques like DPV and chronoamperometry. The method is also illustrated on a cellulose paper strip, projecting its applicability as a naked eye on-spot colorimetric sensor toward the aqueous fluoride ion. The LODs calculated for our approach by UV−vis spectroscopy and DPV techniques are 0.2 and 0.3 ppm. respectively, well below the WHO and BIS limit set for fluoride in drinking water. The methodology is finally tested with environmental samples, and the results corroborated well with the ISE data. The methodology studied can provide a new dimension in the development of a low-cost method for monitoring fluoride ions in drinking water with simple organic probe molecules for low resource world. The work is going on to enrich the methodology toward more impactful application in routine monitoring of fluoride ions in drinking water.

ASSOCIATED CONTENT

Supporting Information

The Supporting Information is available free of charge at https://pubs.acs.org/doi/10.1021/acsomega.4c00624.

Experimental procedures, SCXRD data, spectroscopic data, electron paramagnetic resonance data, voltammetric data, and computational details (PDF)

Accession Codes

CCDC 2313673−2313675 contain the supplementary crystallographic data for this paper. These data can be obtained free of charge via www.ccdc.cam.ac.uk/data_request/cif, or by emailing data_request@ccdc.cam.ac.uk, or by contacting The Cambridge Crystallographic Data Centre, 12 Union Road, Cambridge CB21EZ, UK; fax: +44 1223336033.

AUTHOR INFORMATION

Corresponding Author

Sanjeev Pran Mahanta − *Department of Chemical Sciences, Tezpur University, Tezpur, Assam 784028, India;* orcid.org/0000-0002-7684-8409; Email: spm@tezu.ernet.in, samahanta@gmail.com

https://doi.org/10.1021/acsomega.4c00624
ACS Omega 2024, 9, 29300−29309

Authors

Bikash Chandra Mushahary − *Department of Chemical Sciences, Tezpur University, Tezpur, Assam 784028, India*

Nishant Biswakarma − *Department of Chemical Sciences, Tezpur University, Tezpur, Assam 784028, India*

Ranjit Thakuria − *Department of Chemistry, Gauhati University, Guwahati, Assam 781014, India;* orcid.org/0000-0002-0325-3316

Rituraj Das − *Department of Chemistry, Morigaon College, Morigaon, Assam 782105, India*

Complete contact information is available at: https://pubs.acs.org/10.1021/acsomega.4c00624

Notes

The authors declare no competing financial interest.

■ ACKNOWLEDGMENTS

S.P.M. and B.C.M. acknowledges the Council of Scientific and Industrial Research for funding (project reference number: 01(3000)19EMR-II) and DST-FIST (level-II) programme of Department of Chemical Sciences, Tezpur University. The authors acknowledge SAIC (Tezpur University), SAIF (Gauhati University), NECBH (IITG), and CIF (IITG) for providing instrumental facilities.

■ REFERENCES

(1) Krämer, J.; Kang, R.; Grimm, L. M.; De Cola, L.; Picchetti, P.; Biedermann, F. Molecular probes, chemosensors, and nanosensors for optical detection of biorelevant molecules and ions in aqueous media and biofluids. *Chem. Rev.* **2022**, *122* (3), 3459−3636.

(2) Guo, C.; Sedgwick, A. C.; Hirao, T.; Sessler, J. L. Supramolecular fluorescent sensors: an historical overview and update. *Coord. Chem. Rev.* **2021**, *427*, 213560.

(3) Xu, Z.; Liu, C.; Zhao, S.; Chen, S.; Zhao, Y. Molecular sensors for NMR-based detection. *Chem. Rev.* **2019**, *119* (1), 195−230.

(4) Jagtap, S.; Yenkie, M. K.; Labhsetwar, N.; Rayalu, S. Fluoride in drinking water and defluoridation of water. *Chem. Rev.* **2012**, *112* (4), 2454−2466.

(5) Joshi, S.; Jana, S. Techno-economical assessment of defluoridation of water. *Green Technologies for the Defluoridation of Water*; Elsevier, 2021; pp 175−196..

(6) Johnston, N. R.; Strobel, S. A. Principles of fluoride toxicity and the cellular response: a review. *Arch. Toxicol.* **2020**, *94* (4), 1051−1069.

(7) Carton, R. J.; Park, A. Review of the 2006 United States National Research Council report: fluoride in drinking water. *Fluoride* **2006**, *39* (3), 163−172.

(8) Jurgensen, N.; Petersen, P. E. Promoting oral health of children through schools—results from a WHO global survey 2012. *Community Dent. Health* **2013**, *30* (4), 204−218.

(9) Trieu, A.; Mohamed, A.; Lynch, E. Silver diamine fluoride versus sodium fluoride for arresting dentine caries in children: a systematic review and meta-analysis. *Sci. Rep.* **2019**, *9* (1), 2115.

(10) Featherstone, J. D. Prevention and reversal of dental caries: role of low level fluoride. *Community Dent. Oral Epidemiol.* **1999**, *27* (1), 31−40.

(11) World Health Organization. *Fluoride in Drinking-Water: Background Document for Development of WHO Guidelines for Drinking-Water Quality (No. WHO/HSE/WSH/03.04/96)*; World Health Organization, 2004.

(12) Wiener, R. C.; Shen, C.; Findley, P.; Tan, X.; Sambamoorthi, U. Dental fluorosis over time: a comparison of national health and nutrition examination survey data from 2001−2002 and 2011−2012. *J. Dent. Hyg.* **2018**, *92* (1), 23−29.

(13) Bhagavatula, P.; Curtis, A.; Broffitt, B.; Weber-Gasparoni, K.; Warren, J.; Levy, S. M. The relationships between fluoride intake levels and fluorosis of late-erupting permanent teeth. *J. Public Health Dent.* **2018**, *78* (2), 165−174.

(14) Valdez Jiménez, L.; López Guzmán, O.; Cervantes Flores, M.; Costilla-Salazar, R.; Calderón Hernández, J.; Alcaraz Contreras, Y.; Rocha-Amador, D. O. In utero exposure to fluoride and cognitive development delay in infants. *Neurotoxicology* **2017**, *59*, 65−70.

(15) Grandjean, P. Developmental fluoride neurotoxicity: an updated review. *J. Environ. Health* **2019**, *18* (1), 110.

(16) Perrott, K. W. Fluoridation and attention deficit hyperactivity disorder-a critique of Malin and Till (2015). *Br. Dent. J.* **2017**, *223* (11), 819−822.

(17) Ahmad, S.; Singh, R.; Arfin, T.; Neeti, K. Fluoride contamination, consequences, and removal techniques in water: a review. *Adv. Environ. Sci.* **2022**, *1*, 620−661.

(18) Podgorski, J.; Berg, M. Global analysis and prediction of fluoride in groundwater. *Nat. Commun.* **2022**, *13* (1), 4232.

(19) Lacson, C. F. Z.; Lu, M. C.; Huang, Y. H. Fluoride-containing water: a global perspective and a pursuit to sustainable water defluoridation management—an overview. *J. Clean. Prod.* **2021**, *280*, 124236.

(20) Dhillon, A.; Nair, M.; Kumar, D. Analytical methods for determination and sensing of fluoride in biotic and abiotic sources: a review. *Anal. Methods* **2016**, *8* (27), 5338−5352.

(21) American Public Health Association *Standard Methods for the Examination of Water and Wastewater*; American Public Health Association, 1926; Vol. *6*.

(22) Han, Z.; Wang, K.; Zhou, H. C.; Cheng, P.; Shi, W. Preparation, and quantitative analysis of multicenter luminescence materials for sensing function. *Nat. Protoc.* **2023**, *18* (5), 1621−1640.

(23) Chen, Z.; Lu, Y. L.; Wang, L.; Xu, J.; Zhang, J.; Xu, X.; Cheng, P.; Yang, S.; Shi, W. Efficient recognition, and removal of persistent organic pollutants by a bifunctional molecular material. *J. Am. Chem. Soc.* **2022**, *145* (1), 260−267.

(24) Qiu, Y.; Zhang, Y.; Jiang, Q.; Wang, H.; Liao, Y.; Zhou, H.; Xie, X. Highly specific and sensitive naked-eye fluoride ion recognition via unzipping a helical poly (phenylacetylene). *Macromolecules* **2022**, *55* (20), 9057−9065.

(25) Iizuka, D.; Gon, M.; Tanaka, K.; Chujo, Y. Development of a fluoride-anion sensor based on aggregation of a dye-modified polyhedral oligomeric silsesquioxane. *Chem. Commun.* **2022**, *58* (87), 12184−12187.

(26) Li, Z.; Zhan, D.; Saeed, A.; Zhao, N.; Wang, J.; Xu, W.; Liu, J. Fluoride sensing performance of fluorescent NH 2-MIL-53 (Al): 2D nanosheets vs. 3D bulk. *Dalton Trans.* **2021**, *50* (24), 8540−8548.

(27) Singha, J.; Samanta, T.; Shunmugam, R. Unusual redshift due to selective hydrogen bonding between F-ion and sensor motif: a naked eye colorimetric sensor for F-ions in an aqueous environment. *Mater. Adv.* **2020**, *1* (7), 2346−2356.

(28) Ortiz-Gómez, I.; González-Alfaro, S.; Sánchez-Ruiz, A.; de Orbe-Payá, I.; Capitán-Vallvey, L. F.; Navarro, A.; Salinas-Castillo, A.; García-Martínez, J. C. Reversal of a fluorescent fluoride chemosensor from turn-off to turn-on based on aggregation induced emission properties. *ACS Sens.* **2022**, *7* (1), 37−43.

(29) Zeng, X.; Hu, J.; Zhang, M.; Wang, F.; Wu, L.; Hou, X. Visual detection of fluoride anions using mixed lanthanide metal-organic frameworks with a smartphone. *Anal. Chem.* **2020**, *92* (2), 2097−2102.

(30) Cametti, M.; Rissanen, K. Recognition and sensing of fluoride anion. *Chem. Commun.* **2009**, *20*, 2809−2829.

(31) Zhou, Y.; Zhang, J. F.; Yoon, J. Fluorescence and colorimetric chemosensors for fluoride-ion detection. *Chem. Rev.* **2014**, *114* (10), 5511−5571.

(32) Deng, Z.; Wang, C.; Zhang, H.; Ai, T.; Kou, K. Hydrogen-bonded colorimetric and fluorescence chemosensor for fluoride anion with high selectivity and sensitivity: a review. *Front. Chem.* **2021**, *9*, 666450.

(33) McNeill, A. S.; Stanbury, D. M.; Dixon, D. A. Absolute hydration free energy of small anions and the aqueous pKa of simple acids. *J. Phys. Chem. A* **2022**, *126* (49), 9190−9206.

(34) Miyaji, H.; Sato, W.; Sessler, J. L. Naked-eye detection of anions in dichloromethane: colorimetric anion sensors based on calix [4] pyrrole. *Angew. Chem., Int. Ed.* **2000**, *39* (10), 1777−1780.
(35) Amendola, V.; Esteban-Gómez, D.; Fabbrizzi, L.; Licchelli, M. What anions do to N-H-containing receptors. *Acc. Chem. Res.* **2006**, *39* (5), 343−353.
(36) Jose, D. A.; Kumar, D. K.; Ganguly, B.; Das, A. Efficient and simple colorimetric fluoride ion sensor based on receptors having urea and thiourea binding sites. *Org. Lett.* **2004**, *6* (20), 3445−3448.
(37) Mahanta, S. P.; Kumar, B. S.; Baskaran, S.; Sivasankar, C.; Panda, P. K. Colorimetric sensing of fluoride ion by new expanded calix [4] pyrrole through anion-π interaction. *Org. Lett.* **2012**, *14* (2), 548−551.
(38) Mahanta, S. P.; Panda, P. K. Bis (pyrrole-benzimidazole) conjugates as novel colorimetric sensor for anions. *J. Chem. Sci.* **2017**, *129*, 647−656.
(39) Bose, P.; Ahamed, B. N.; Ghosh, P. Functionalized guanidinium chloride based colourimetric sensors for fluoride and acetate: single crystal X-ray structural evidence of-NH deprotonation and complexation. *Org. Biomol. Chem.* **2011**, *9* (6), 1972−1979.
(40) Duke, R. M.; O'Brien, J. E.; McCabe, T.; Gunnlaugsson, T. Colorimetric sensing of anions in aqueous solution using a charge neutral, cleft-like, amidothiourea receptor: tilting the balance between hydrogen bonding and deprotonation in anion recognition. *Org. Biomol. Chem.* **2008**, *6* (22), 4089−4092.
(41) Das, R.; Talukdar, D.; Sarma, P. J.; Kuilya, H.; Thakuria, R.; Choudhury, D.; Mahanta, S. P. Colorimetric detection of fluoride ions in aqueous medium using thiourea derivatives: a transition metal ion assisted approach. *Dalton Trans.* **2021**, *50* (42), 15287−15295.
(42) Stauber, J. M.; Alliger, G.; Nocera, D. G.; Cummins, C. C. Second-coordination-sphere assisted selective colorimetric turn-on fluoride sensing by a mono-metallic Co (II) hexacarboxamide cryptand complex. *Inorg. Chem.* **2017**, *56* (14), 7615−7619.
(43) Das, R.; Sarma, P. J.; Borborah, A.; Bharati, S. P.; Mahanta, S. P. Revisiting the fluoride binding behaviour of dipyrrolylquinoxaline in aqueous medium: a copper ion mediated approach. *New J. Chem.* **2019**, *43* (8), 3447−3453.
(44) Sarkar, A.; Bhattacharyya, S.; Mukherjee, A. Colorimetric detection of fluoride ions by anthraimidazoledione based sensors in the presence of Cu (II) ions. *Dalton Trans.* **2016**, *45* (3), 1166−1175.
(45) Hendricks, M. P.; Campos, M. P.; Cleveland, G. T.; Jen-La Plante, I.; Owen, J. S. A tunable library of substituted thiourea precursors to metal sulfide nanocrystals. *Science* **2015**, *348* (6240), 1226−1230.
(46) Benesi, H. A.; Hildebrand, J. H. J. A spectrophotometric investigation of the interaction of iodine with aromatic hydrocarbons. *J. Am. Chem. Soc.* **1949**, *71* (8), 2703−2707.
(47) Armbruster, D. A.; Pry, T. Limit of blank, limit of detection and limit of quantitation. *Clin. Biochem. Rev.* **2008**, *29*, S49−S52.
(48) Nakamoto, K. *Infrared and Raman Spectra of Inorganic and Coordination Compounds, Part B: Applications in Coordination, Organometallic, and Bioinorganic Chemistry*; John Wiley & Sons, 2009.
(49) Frisch, M. E.; Trucks, G. W.; Schlegel, H. B.; Scuseria, G. E.; Robb, M. A.; Cheeseman, J. R.; Fox, D. J. *Gaussian 16*. Revision C. 01, 2016.
(50) Adamo, C.; Jacquemin, D. The calculations of excited-state properties with time-dependent density functional theory. *Chem. Soc. Rev.* **2013**, *42* (3), 845−856.
(51) Takano, Y.; Houk, K. N. Benchmarking the conductor-like polarizable continuum model (CPCM) for aqueous solvation free energies of neutral and ionic organic molecules. *J. Chem. Theory Comput.* **2005**, *1* (1), 70−77.
(52) Cossi, M.; Rega, N.; Scalmani, G.; Barone, V. Energies, structures, and electronic properties of molecules in solution with the C-PCM solvation model. *J. Comput. Chem.* **2003**, *24* (6), 669−681.
(53) Zhang, Y. C.; Chilukuri, B.; Hanson, T. B.; Heiden, Z. M.; Lee, D. Y. Connecting solution-phase to single-molecule properties of Ni (salophen). *J. Phys. Chem. Lett.* **2019**, *10* (13), 3525−3530.
(54) Tang, H. M.; Fan, W. Y. Dithiolato-bridged nickel (II) salicylcysteamine complexes as robust proton reduction electrocatalysts: cyclic voltammetry and computational studies. *Inorg. Chem.* **2021**, *60* (23), 17933−17941.
(55) Maity, D.; Bhaumik, C.; Mondal, D.; Baitalik, S. Ru (II) and Os (II) complexes based on terpyridyl-imidazole ligand rigidly linked to pyrene: synthesis, structure, photophysics, electrochemistry, and anion-sensing studies. *Inorg. Chem.* **2013**, *52* (24), 13941−13955.
(56) Dhawan, S.; Devnani, H.; Babu, J.; Singh, H.; Haider, M. A.; Khan, T. S.; Ingole, P. P.; Haridas, V. Supersensitive detection of anions in pure organic and aqueous media by amino acid conjugated Ellman's reagent. *ACS Appl. Bio Mater.* **2021**, *4* (3), 2453−2464.
(57) Mahishi, A. A.; Shet, S. M.; Mane, P. V.; Yu, J.; Sowriraajan, A. V.; Kigga, M.; Bhat, M. P.; Lee, K. H.; Kurkuri, M. D. Ratiometric colorimetric detection of fluoride ions using a Schiff base sensor: enhancing selectivity and sensitivity for naked-eye analysis. *Anal. Methods* **2023**, *15* (26), 3259−3267.
(58) Wu, X.; Wang, H.; Yang, S.; Tian, H.; Liu, Y.; Sun, B. Highly sensitive ratiometric fluorescent paper sensors for the detection of fluoride ions. *ACS Omega* **2019**, *4* (3), 4918−4926.

https://doi.org/10.1021/acsomega.4c00624
ACS Omega 2024, 9, 29300−29309